Synthesis, Chemical−Physical Characterization, and Redox Properties of a New Mixed-Ligand Heterobimetallic N-Bridged Dimer: (μ-Nitrido)[((tetraphenylporphyrinato)manganese)((phthalocyaninato)iron)]

Maria Pia Donzello,[†] Claudio Ercolani,*[,†] Karl M. Kadish,*[,‡] Zhongping Ou,[‡] and Umberto Russo[§]

Dipartimento di Chimica, Università degli Studi di Roma "La Sapienza", Roma, Italy, Department of Chemistry, University of Houston, Houston, Texas 77204-5641, and Dipartimento di Chimica Inorganica, Metallorganica, ed Analitica, Università degli Studi di Padova, Padova, Italy

Received December 17, 1997

A new mixed-ligand heterobimetallic μ-nitrido bridged complex of the formula (TPP)Mn−N−Fe(Pc) (**I**) has been prepared from (TPP)MnN_3 and (Pc)Fe (TPP = tetraphenylporphyrinato anion, Pc = phthalocyaninato anion) and its molecular and electronic structure were investigated by EPR, IR, Raman, UV−visible and Mössbauer spectroscopy as well as by electrochemistry and magnetic susceptibility measurements. The complex, formally a mixed-valence Mn−Fe d^8 system, is low-spin (diamagnetic). Mössbauer data indicate an unbalanced positive charge distribution for the two metal centers and an approach to the formally mixed-valence species (TPP)-Mn^{IV}=N−Fe^{III}(Pc). This assignment differs from findings for the related complex (TPP)$Fe^{III1/2}$−N−$Fe^{III1/2}$(Pc) (**II**) and other similar N-bridged analogues, including (TPP)Fe^{IV}=N−Ru^{III}(Pc). A metal centered one-electron oxidation occurs by reaction of **I** with dilute $HClO_4$ and leads to formation of a Mn(IV)=N−Fe(IV) species, **I**-ClO_4. Pyridine can coordinate with **I** to give a mono(pyridine) adduct and the formation constant for this reaction has been determined spectrophotometrically in CH_2Cl_2 solutions. The singly oxidized complex, **I**-ClO_4, also reacts with pyridine and is converted to a bis-pyridine derivative containing the fragment [(py)(TPP)Mn−N−Fe(Pc)(py)]$^+$. Complex **I** can undergo five reversible one-electron oxidations in CH_2Cl_2 and up to six electrons can be extracted from the neutral complex in pyridine. Both sets of reactions were characterized by cyclic voltammetry which was used to determine the half-wave potentials for each electrode reaction and also to evaluate formation constants for pyridine binding to the neutral and singly oxidized forms of the complex.

Introduction

It has long been known that bimetallic, formally mixed valence Fe(III)−Fe(IV) species of the type (TPP)Fe−N−Fe(TPP)[1,2] and (Pc)Fe−N−Fe(Pc)[3] undergo a rapid electronic exchange across the bridging N-atom so that both metal centers can be assigned an intermediate average oxidation state of 3.5. A similar exchange and average oxidation state of 3.5 can also be seen for N-bridged bimetallic complexes containing the same metal ion and two different macrocycles as was more recently demonstrated for (TPP)Fe−N−Fe(Pc).[4] This contrasts with what is observed for the Fe−Ru analogue of the same compound, i.e., (TPP)Fe−N−Ru(Pc),[5] where the two metal centers show distinct oxidation states and the complex is formulated as (TPP)Fe^{IV}=N−Ru^{III}(Pc).

Differences in electron distribution between the diiron and mixed Fe−Ru μ-nitrido dimers are also seen in the singly oxidized forms of the complexes. The electrochemical or chemical oxidation of (TPP)Fe−N−Fe(TPP), (Pc)Fe−N−Fe(Pc), and (TPP)Fe−N−Fe(Pc) by one electron occurs at the metal center to yield a derivative with two equivalent Fe(IV) atoms,[1−4] whereas the chemical one-electron oxidation of the Fe−Ru analogue occurs at the macrocycle leading to formation of a species formulated as [(TPP)Fe^{IV}=N−Ru^{III}(Pc)]$^{\bullet+}$.[4]

We now report the second example of a mixed macrocycle bimetallic N-bridged complex containing two different metal centers. This compound, formally formulated as (TPP)Mn−N−Fe(Pc), is characterized in the present paper by EPR, IR, Raman, UV−visible, and Mössbauer spectroscopy as well as by magnetic susceptibility measurements. Its chemical and electrochemical behavior are also examined, and the combined data are used to assign each metal oxidation state in both the neutral and singly oxidized forms of the complex. As will be shown, the electronic distribution in neutral (TPP)Mn−N−Fe(Pc) differs from that of the above-mentioned species, and this difference is also seen for the chemical and electrochemical reactivity of these species.

Experimental Section

Chemicals. THF, DMF, acetone, hexane, CH_2Cl_2, $CHCl_3$, pyridine, PhCN, ClNP, hydrazine monohydrate, $HClO_4$, tetra-*n*-butylammonium perchlorate (TBAP), CaH_2, and $NaBH_4$ were all pure solvents or chemicals (Carlo Erba or Aldrich) and were used as received unless

[†] Università degli Studi di Roma "La Sapienza".
[‡] University of Houston.
[§] Università degli Studi di Padova.

(1) Kadish, K. M.; Rhodes, R. K.; Bottomley; L. A.; Goff, H. M. *Inorg. Chem.* **1981**, *20*, 3195 and references therein. Abbreviations used in the present paper: Pc = phthalocyaninato anion; TPP = tetraphenylporphyrinato anion; THF = tetrahydrofuran; DMF dimethyl formamide; PhCN = benzonitrile; ClNP = α-chloronaphthalene.
(2) Bottomley, L. A.; Gorce, Jean-Noel; Goedken, V. L.; Ercolani, C. *Inorg. Chem.* **1985**, *24*, 3733 and references therein.
(3) Ercolani, C.; Hewage, S.; Heucher, R., and Rossi, G. *Inorg. Chem.* **1992**, *32*, 2975.
(4) Ercolani, C.; Jubb, J.; Pennesi, G.; Russo, U.; Trigiante, G. *Inorg. Chem.* **1995**, *34*, 2535.
(5) Ercolani, C.; B. Floris, *Phthalocyanines-Properties and Applications*; Leznoff, C. C., Lever, A. B. P., Eds; VCH Publishers: New York, 1993; Vol. 2, pp 1−42.

S0020-1669(97)01585-1 CCC: $15.00
Published on Web 07/01/1998

otherwise indicated (see below). $Na^{15}NO_2$ (99% ^{15}N) was purchased from Matheson. (Pc)Fe was purchased from Eastman Kodak, and its purity verified by elemental analysis and room-temperature magnetic moment measurements; if necessary, it was purified by sublimation under vacuum (400−450 °C, 10^{-2} mmHg). (TPP)MnN_3 was prepared following a reported procedure[6] and purified by crystallization from a $CHCl_3$−hexane mixture. ClNP was refluxed in the presence of CaH_2 and freshly distilled before use. For electrochemical measurements, PhCN was distilled over P_2O_5 and TBAP was recrystallized from ethyl alcohol and dried under vacuum at 40 °C for at least 1 week prior to use.

[(TPP)Mn−N−Fe(Pc)] (I). (TPP)MnN_3 (1.28 g, 1.80 mmol) and (Pc)Fe (0.73 g, 1.28 mmol) (molar ratio 1.4:1) were suspended (partly dissolved) in anhydrous freshly distilled ClNP (35 mL). The mixture was heated at 140 °C in an inert atmosphere (N_2) for 21 h with stirring. After cooling and filtration, the solid separated material was washed abundantly with hexane, after which it was brought to constant weight under vacuum (1.54 g). The crude material was suspended in 1.25 L of CH_2Cl_2, and the resulting clear solution was separated from the undissolved material (predominantly residual unreacted (Pc)Fe) by filtration. The solid which was isolated after evaporation of the solvent (ca. 1.03 g) still contained traces of (Pc)Fe (as evidenced by a characteristic UV−visible band at 654 nm), and elimination of this (Pc)Fe impurity was accomplished by repeatedly suspending the solid material in aliquots of pyridine until the color of the solution changed from deep green to brown, followed by washing the solid with a small amount of CH_2Cl_2 to eliminate the pyridine. The solid was then brought to a constant weight by heating under vacuum (10^{-2} mmHg) at 220 °C for 2.5 h (847 mg, yield 53%). The completion of the reaction to give **I** was ascertained by monitoring the disappearance of an intense vibration band located at ca. 2030 cm^{-1} due to the azide group of the starting (TPP)MnN_3.

The brownish-black solid complex is indefinitely stable in air. Thermogravimetric analysis shows no weight loss up to temperatures of 300−350 °C, and the IR spectrum of the residue indicates that the material is practically unchanged after heating. Anal. Calcd for **I,** $C_{76}H_{44}FeMnN_{13}$: C, 73.02; H, 3.55; N, 14.57; Fe, 4.47; Mn, 4.39. Found: C, 72.87; H, 3.30; N, 14.09; Fe, 4.24; Mn, 4.15.

Isotopically ^{15}N-Enriched [(TPP)Mn−$^{15(50\%)}$N−Fe(Pc)] (Ia). Isotopically enriched NaN_3 was prepared by following a standard reported procedure.[7] $Na^{15}NO_2$ (99% ^{15}N) was converted into *n*-butyl-O^{15}NO, followed by reaction with hydrazine monohydrate, to give isotopically enriched NaN_3 in which one of the two external N atoms of the N_3^- ion is ^{15}N. A reaction of this species with (TPP)$MnOCOCH_3$ gives two types of (TPP)MnN_3 products as expected; one is (TPP)Mn−(^{15}N−^{14}N−^{14}N) (**A**), and the other, (TPP)Mn−(^{14}N−^{14}N−^{15}N) (**B**). The generation of this isotopic mixture was confirmed by measuring the IR spectrum of enriched (TPP)MnN_3, which showed two distinct azide group absorptions at 2027 and 2015 cm^{-1}. A reaction of (Pc)Fe with the isotopic mixture of **A** and **B** was expected to give **I** containing equivalent amounts of (TPP)Mn−^{15}N−Fe(Pc) and (TPP)Mn−^{14}N−Fe(Pc), and this is the case as described in following sections of the manuscript.

[(TPP)Fe−N−Fe(Pc)] (II). This species was obtained from (TPP)-FeN_3 and (Pc)Fe as described in the literature.[3]

[(TPP)Mn−N−Fe(Pc)(py)] (I-py). The mono(pyridine) adduct was quantitatively obtained by dissolving **I** (56.8 mg) in pyridine (73 mL) followed, after 3.5 h, by complete evaporation of the solvent. The obtained dark gray solid was brought to a constant weight under vacuum (10^{-2} mmHg). Anal. Calcd for I-py: C, 73.20; H, 3.72; N, 14.75. Found: C, 73.21; H, 3.93; N, 13.96. Thermogravimetric analysis of the complex showed a weight loss of 5.63% at 100−130 °C, and this is consistent with the calculated weight loss of 5.95% for 1 molecule of pyridine.

Oxidation of I with $HClO_4$ To Give a Perchlorate Product (I-ClO_4) and Conversion of This Oxidized Species to a Bis(pyridine) Derivative, [(py)(TPP)Mn−N−Fe(Pc)(py)](ClO_4), [I-(py)$_2$](ClO_4). All attempts to oxidize **I** using dilute aqueous $HClO_4$ (10%) in THF or DMF were unsuccessful, and the initial compound remained intact. However, samples of **I** containing trace impurities of (Pc)Fe were observed to undergo an oxidation in DMF. This result suggests that (Pc)Fe catalyzes the oxidation to give a final material which shows an irreproducible retention of solvent molecules. As a result, elemental analyses do not lead to a plausible formulation of the species. However, IR and EPR results (see the following sections) clearly indicate that an oxidation has taken place and that some type of mono(perchlorate) product, formulated as **I**-ClO_4, is formed. When **I**-ClO_4 is suspended in benzene containing excess of $NaBH_4$ at room temperature, it is reduced to **I** as indicated by its characteristic IR spectrum.

A sample of **I**-ClO_4 was suspended in a mixture of acetone and pyridine and then stirred for 2 h at room temperature. After substantial evaporation of the solvent mixture, the solid was separated by filtration, washed with acetone, and brought to a constant weight under vacuum. Elemental analysis suggests formation of a bis(pyridine) derivative having the formula [(py)(TPP)Mn−N−Fe(Pc)(py)](ClO_4). Anal. Calcd for **[I**-(py)$_2$]ClO_4, $C_{86}H_{54}ClFeMnN_{15}O_4$: C, 68.51; H, 3.61; N, 13.93. Found: C, 68.17; H, 3.84; N, 13.52.

[(TPP)Fe−N−Fe(Pc)](ClO_4) (II-ClO_4). Complex **II** (83 mg, 0.066 mmol) was suspended in DMF (9 mL) containing excess TBAP and 1.5 mL perchloric acid (10%) and stirred at room temperature for 20 h. After filtration, the separated solid was washed abundantly with water and brought to a constant weight under vacuum (64 mg). The exact formulation of the final product was associated with problems very similar to those described above for the corresponding Mn−Fe perchlorate formed after oxidaiton of the initial compound. Additional characterization of **II**-ClO_4 is given in later sections of the manuscript.

Cyclic Voltammetric and Spectroelectrochemical Instrumentation. Cyclic voltammetry was carried out with an EG&G model 173 potentiostat or an IBM Model EC 225 voltammetric analyzer. Current−voltage curves were recorded on an EG&G Princeton Applied Research model R-0151 X-Y recorder. A three-electrode system was used and consisted of a glassy carbon or platinum button working electrode, a platinum wire counter electrode, and a saturated calomel reference electrode (SCE). This reference electrode was separated from the bulk of the solution by a fritted glass bridge filled with the solvent/supporting electrolyte mixture. All potentials are referenced to the SCE. UV−visible spectroelectrochemical experiments were performed by using an HP 8453 UV−visible spectrophotometer, with a home-built platinum thin-layer cell of the type described in the literature.[8] Potentials were applied and monitored with an EG&G Princeton Applied Research model 173 potentiostat.

Other Physical Measurements. IR spectra in the region 4000−200 cm^{-1} were recorded on a Perkin-Elmer 783 instrument by using Nujol mulls between CsI windows. UV−visible solution spectra of **I** in CH_2Cl_2 containing variable amounts of pyridine were obtained with a Varian Cary 5E spectrometer. Room-temperature magnetic susceptibility measurements were obtained by the Gouy method on a permanent magnet (7000 G) using a $NiCl_2$ solution as calibrant. The diamagnetic contribution of the macrocycles was chosen as -386×10^{-6} and -430×10^{-6} cgsu/mol for the TPP and Pc ligands, respectively. Mössbauer spectra were obtained as described elsewhere.[9] EPR spectra were recorded on a Varian V4502-4 spectrometer (X-band). Raman spectra were run on a Spex Triplemate model 1877 spectrograph equipped with a cooled EG&G Parc model 1454 OMA detector. FAB experiments were carried out on a multiple quadrupole instrument (VG quattro). Thermogravimetric analyses were performed on a Stanton Redcroft model STA-781 analyzer under an N_2 atmosphere. Elemental analyses for C, H, and N were made at the University of Rome on an EA 1110 CHNS-O CE instrument. Fe and Mn were quantitatively detected by atomic absorption on a Varian Spectra AA-30.

(6) Schardt, B. C.; Hollander, F. J.; Hill, C. L. *J. Am. Chem. Soc.* **1982**, *104*, 3964.
(7) Miller, M. V.; Audrieth, L. F. *Inorganic Syntheses*; McGraw-Hill: New York, Vol. 2, 1946; p 139.
(8) Lin, X. Q.; Kadish, K. M. *Anal. Chem.* **1985**, *57*, 1498.
(9) Ercolani, C.; Gardini, M.; Pennesi, G.; Rossi, G.; Russo, U. *Inorg. Chem.* **1988**, *27*, 422.

Table 1. Low-Temperature (78 K) Mössbauer Data for **I** and Other Related Species

no.	complex	δ^a (mm s^{-1})	ΔE_Q (mm s^{-1})	Γ^b (mm s^{-1})	refs^c
1	[(Pc)Fe^{III}]$_2$O (μ-Oxo(2)]	0.26	1.26	0.14	14
2	(TPP)Mn−N−Fe(Pc) (**I**)	0.19	1.21	0.13	tp
3	**I**-py	0.12	1.30	0.17	tp
4	[(Pc)Fe$^{III1/2}$]$_2$N	0.06	1.76	0.19	3
5	(TPP)Fe$^{III1/2}$−N− Fe$^{III1/2}$(Pc) (**II**)	0.11	1.47	0.19	4
6	[(TPP)Fe$^{III1/2}$]$_2$N^d	0.18	1.08		12
7	[(Pc)Fe^{IV}]$_2$C	−0.16	2.69	0.11	13
8	[(TPP)Fe^{IV}]$_2$C^d	0.10	1.88		12
9	(TPP)Fe^{IV}=N−Ru^{III}(Pc)	0.03	0.90	0.22	4
10	[(TPP)Fe^{IV}=N−Ru^{III}(Pc)]$^{\bullet+}$	−0.01	1.85	0.23	4
11	**I**-ClO_4 (34%)	−0.02	2.64	0.25	tp
11′	**I**-ClO_4 (29%)	0.00	1.99	0.24	
11″	**I**-ClO_4 (37%)	−0.01	1.29	0.25	
12	[**I**-(py)$_2$]ClO_4	0.02	1.37	0.25	tp
13	**II**-ClO_4	−0.11	1.94	0.22	tp

[a] Referred to metallic iron. [b] Half-width at half maximum height. [c] tp = this paper. [d] Data taken at 131 K.

Results and Discussion

The following discussion concerns aspects associated with the synthesis of **I,** its chemical and physical characterization, and its redox properties.

(i) Synthetic Aspects. The reaction must be carried out under an inert atmosphere to prevent formation of [(Pc)Fe]$_2$O in the presence of molecular oxygen. The temperature must also be accurately fixed over a narrow range around 140 °C in order for the reaction to proceed. Temperatures lower than 140 °C invariably lead to an incomplete reaction, while higher temperatures (160−170 °C) result in a different reaction pathway such that up to 80% of the initial (Pc)Fe is converted to [(Pc)Fe]$_2$N rather than (TPP)Mn−N−Fe(Pc).

The formation of [(Pc)Fe]$_2$N most likely involves an azide group shift during the reaction, leading to an unstable (Pc)FeN$_3$ intermediate that can react with (Pc)Fe to give [(Pc)Fe]$_2$N. A loss of the azide group from (TPP)FeN$_3$ is also observed in reaction of the compound with (Pc)Fe under similar experimental conditions, and this is followed again by conversion of the (Pc)FeN$_3$ intermediate to a final [(Pc)Fe]$_2$N product.[4]

A few crystals of (TPP)MnCl were often isolated in the form of brown needles from the residual ClNP solution at the end of the reaction. A few prismatic crystals were also occasionally isolated and probably consisted of a (TPP)MnCl complex which is solvated with ClNP, as indicated by elemental analyses and IR spectra. The formation of (TPP)MnCl from (TPP)MnN$_3$ can be explained simply by assuming loss of the azide group followed by chlorine abstraction from ClNP. A similar abstraction process is observed for (Pc)Fe in ClNP containing I_2. The product of this latter reaction is (Pc)FeCl as demonstrated by the fortuitous isolation of crystals which were identified by single-crystal X-ray analysis as the iodine-bridged complex, (Pc)FeCl−I_2−ClFe(Pc).[10]

Iron and manganese elemental analyses were systematically performed in order to unequivocally identify formation of the N-bridged bimetallic complex **I**. FAB experiments show clearly the molecular peak of **I** accompanied by peaks for the fragments (TPP)MnN and (Pc)Fe. Thermogravimetric analysis shows **I** to undergo no weight loss up to temperatures of 300−350 °C, thus confirming the lack of coordinated water or other ligated molecules, consistent with results from the IR data.

(ii) Chemical−Physical Characterization. Magnetic Susceptibility and EPR Data. The two metal centers of complex **I** have a total number of 8 d electrons and a +7 charge whatever the charge distribution, and this is counterbalanced by a negative charge of −4 arising from the two macrocyclic ligands and −3 from the single bridging N atom. Room-temperature magnetic susceptibility measurements show **I** to have a μ_{eff} value of 0.5−1.0 μ_B which corresponds to a very low paramagnetism, and this can be reasonably accounted for by the presence of trace amounts of paramagnetic contaminants. Magnetic susceptibility results indicate complete spin pairing, which is also supported by the fact that compound **I** is EPR silent. A low-spin electronic structure for I is not surprising; although there appears to be no information in the literature about μ-nitrido Mn−Fe species, a low-spin configuration has been established for several μ-nitrido Fe−Fe analogues.[11] One can therefore confidently conclude that **I** is a low-spin d^8 system.

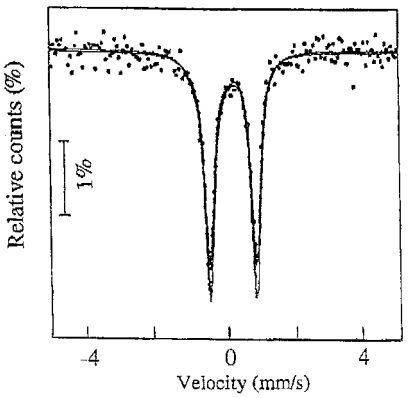

Figure 1. Low-temperature (78 K) Mössbauer spectrum of **I**.

Mössbauer Data. The Mössbauer spectrum of **I** (Figure 1) shows a single well-resolved doublet indicating the presence of only one type of Fe center. Its isomer shift and quadrupole splitting values (0.19 and 1.21 mm s^{-1}, respectively) are given in Table 1 (complex **2**) together with values of several closely related species which are listed according to the increasing oxidation state of the Fe centers. As seen in the table, the isomer shift of **I** is higher than isomer shifts of the related μ-nitrido species **4**−**6**, each of which has two Fe centers with equivalent intermediate oxidation states of +3.5. The isomer shift of **I** is also much higher than the isomer shifts of related species which contain either two equivalent Fe(IV) atoms (**7**, **8**) or a single Fe(IV) atom (**9**, **10**).

The dependence of δ upon the nature of the two macrocyclic ligands is evident within the series of the N-bridged compounds

(10) Palmer, S. M.; Stanton, J. L.; Jaggi, N. K.; Hoffman, B. M.; Ibers, J. A. *Inorg. Chem.* **1985**, *24*, 2040.

(11) Justel, T.; Weyhermüller, T.; Wieghardt, K.; Bill, E.; Lengen, M.; Trautwein, A. X.; Hildebrandt, P. *Angew. Chem., Int. Ed. Engl.* **1995**, *34*, 669 and references therein.

4−**6**. The data indicate, for instance, that lower δ values are seen as the number of Pc groups in the complex is increased; for example, $\delta = 0.18$ mm s^{-1} in the case of [(TPP)Fe]$_2$N (complex **6**), 0.11 mm s^{-1} in the case of (TPP)Fe−N−Fe(Pc) (**II**, complex **5**), and 0.06 mm s^{-1} in the case of [(Pc)Fe]$_2$N (complex **4**). A similar trend in δ is observed for the μ-carbido species [(TPP)Fe]$_2$C (complex **8**) and [(Pc)Fe]$_2$C (complex **7**). Noticeably, opposite changes are observed for the ΔE_Q values in both series **4**−**6** and **7** and **8**.

A comparison of the δ values of **I** and **II** is of particular interest since the two complexes differ only by the central metal on the TPP macrocycle. The δ value is higher for **I**, and this seems to suggest a less balanced positive charge distribution for the heterobimetallic site with a more pronounced approach of the Fe center to an oxidation state of +3. This is clearly ascribable to the presence in **I** of the Mn ion which has a high tendency to attain a +4 oxidation state. In the extreme occurrence, a mixed valence Mn(IV)−Fe(III) couple would be formed in (TPP)Mn^{IV}=N−Fe^{III}(Pc), which would have double and single bonds located at the Mn−N and N−Fe sites, respectively.

It is noteworthy to point out that the observed δ value for **I** is somewhat lower but not far away from the 0.26 mm s^{-1} value found for the μ-oxo species [(Pc)Fe]$_2$O (μ-Oxo(2))[14] (complex **1** in Table 1) which contains two equivalent Fe(III) atoms. Fe(III) is also present in the μ-oxo-TPP analogue, [(TPP)Fe]$_2$O, which exhibits a considerably higher δ value (0.40 mm s^{-1}).[12] In this case, however, the observed increment can be entirely ascribed to the presence of two TPP macrocycles in the dimer, in line with previous observations for species **4**−**6** and **7** and **8**.

The above proposed unbalanced charge distribution on the metal centers of **I** is not only different from that of complex **II**, which contains two equivalent Fe(III1/2) centers, but it is opposite to that of the Fe−Ru complex (complex **9** in Table 1), in which the Fe and Ru centers have been shown to exist in +4 and +3 oxidation states, respectively.[4] As will be shown, these two different mixed-ligand Mn−Fe and Fe−Ru systems also have a different charge distribution after being oxidized by one electron to give the singly oxidized product.

IR and Raman Spectra. The IR and Raman spectra of **I** and **II** are quite similar to each other in the spectral region 4000−200 cm^{-1} since both species exhibit TPP and Pc modes. Spectral differences between the two compounds are almost exclusively due to modes of the M−N−M bond system, which are located in the regions 1000−900 and 400−350 cm^{-1}. The only exception is the presence of one medium-to-strong absorption which is present at 1040 cm^{-1} in the Raman spectrum of **I** but not observed in the corresponding IR spectrum of this compound. This band is also absent in the Raman and IR spectrum of **II**, and we are presently unable to explain its origin.

An intense IR absorption is seen for complex **II** at 930 cm^{-1} (Figure 2, arrow), and this absorption was previously assigned as ν_{as}(Fe−N−Fe).[4] Similar assignments were made for [(Pc)Fe]$_2$N (915 cm^{-1}),[2] [(TPP)Fe]$_2$N (910, 885 cm^{-1}),[6] and the μ-carbido species, [(TPP)Fe]$_2$C (ν_{as}(Fe−C−Fe); 940 and 885 (sh) cm^{-1}).[15] This has been taken as indicating a considerable

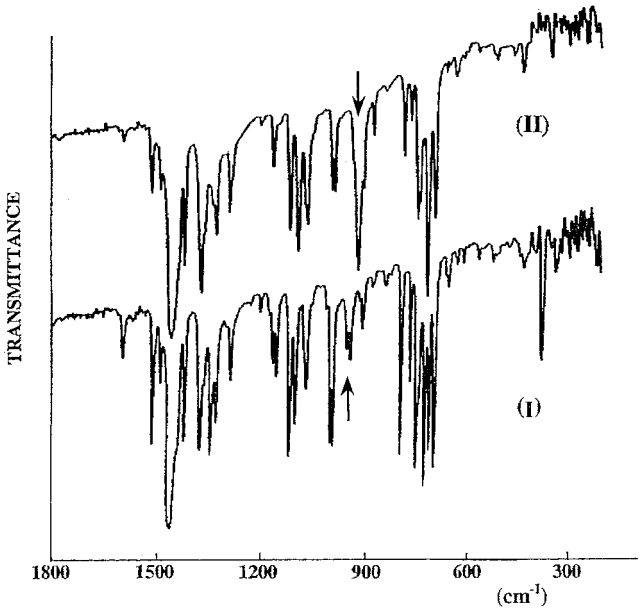

Figure 2. Nujol mull IR spectra of **I** and **II** in the IR region 1800−200 cm^{-1}.

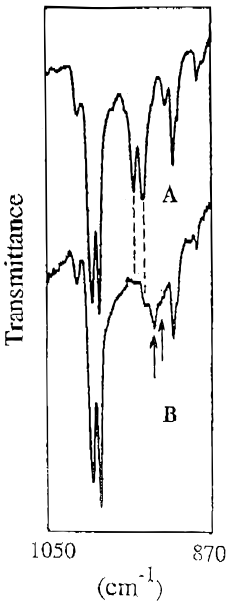

Figure 3. Nujol mull IR spectra of **I** (A) and ^{15}N isotopically enriched **I** (B) in the region 1050−870 cm^{-1}.

degree of π-bond character in the linear Fe−X−Fe moiety. A linearity in the triatomic bridge is strongly suggested by the general information available on these kinds of μ-nitrido and μ-carbido Fe−X−Fe bonded systems (X = N, C), including single-crystal X-ray structural work on some analogues[16] and a closely related complex, [(THF)(TPP)Fe−N−Fe(Pc)(H$_2$O)](I$_5$)·2THF.[4] The ν_{as} stretching mode for **II** is completely absent in the corresponding Raman spectrum (Figure 4), which is in line with expectation (ν_{as} is IR active but Raman inactive) and confirms the previous assignment.

The IR spectrum of **I** shows a weak doublet in the 1000−900 cm^{-1} region, with peaks at 956 and 945 cm^{-1} (indicated

(12) English, R.; Hendrikson, D. N.; Suslick, K. S. *Inorg. Chem.* **1983**, *22*, 367.
(13) (a) Ercolani, C.; Gardini, M.; Goedken, V. L.; Pennesi, G.; Rossi, G.; Russo, U.; Zanonato, P. *Inorg. Chem.* **1989**, *28*, 3097. (b) Bakshi, E. N.; Delfs, C. D.; Murray, K. S.; Peters, B.; Homborg, H. *Inorg. Chem.* **1988**, *27*, 4318.
(14) Ercolani, C.; Gardini, M.; Murray, K. S.; Pennesi, G.; Rossi, G. *Inorg. Chem.* **1987**, *26*, 3539.
(15) Mansuy, D.; Lecomte, J.-P.; Chottard, J.-C.; Bartoli, J.-F. *Inorg. Chem.* **1981**, *20*, 3119.
(16) (a) Scheidt, W. R.; Summerville, D. A.; Cohen, I. A. *J. Am. Chem. Soc.* **1976**, *98*, 6623. (b) Rossi, G.; Goedken, V. L.; Ercolani, C. *J. Chem. Soc., Chem. Commun.* **1988**, 46. (c) Moubaraki, P. B.; Benlian, D.; Baldy, A.; Pierrot, M. *Acta Crystallogr.* **1989**, *C45*, 393.

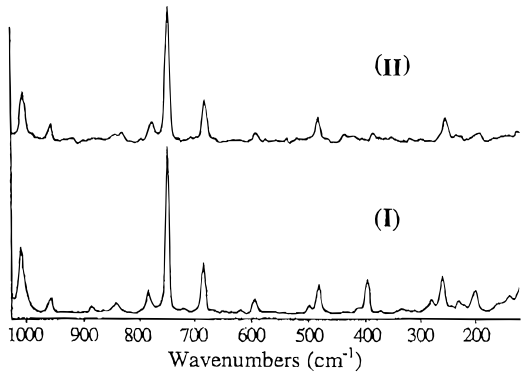

Figure 4. Raman spectra of **I** and **II** in the region 1020−120 cm^{-1}.

by an arrow in Figure 2). An unequivocal assignment of this doublet as ν_{as}(Mn−N−Fe) can be made on the basis of the IR spectral changes observed upon ^{15}N isotopic enrichment of the central N bridging atom. The spectrum of **I** and that for a sample of this species consisting of approximately equal amounts of (TPP)Mn−^{15}N−Fe(Pc) and (TPP)Mn−^{14}N−Fe(Pc) (Figure 3) shows that upon going from **I** to the isotopically enriched species, the original doublet (Figure 3A, average position ∼ 950 cm^{-1}) decreases in intensity and a new weak doublet appears at 933 and 923 cm^{-1} (Figure 3B, average position ∼928 cm^{-1}), leaving the other peaks (1000, 992, and 911 cm^{-1}) unchanged. The magnitude of the observed shift to lower frequencies of the original doublet (∼22 cm^{-1}) is roughly that which is expected in light of the assignment made for such types of isotopic ^{15}N substitution.[17] (See, for instance, a similar case[18] for [(Pc)Ru]$_2$N: 27 cm^{-1}). In keeping with expectation, the doublet is absent in the corresponding Raman spectrum of **I** (Figure 4); the weak absorption found at 957 cm^{-1} for **I** must, in fact, have a different assignment, since it is also present in the Raman spectrum of **II** (Figure 4).

The ν_s(M−N−M) mode is expected to appear in the low-frequency range (450−300 cm^{-1}) of the Raman spectrum (IR inactive), and this stretching mode has been identified for [(TPP)Fe]$_2$N at 424 cm^{-1}, a value which is shifted by 6 cm^{-1} toward higher frequency upon ^{54}Fe isotopic substitution.[19] A comparison of the spectral data for species **I** and **II** shows the following: (a) No bands attributable to ν_s(Fe−N−Fe) could be detected for **II** in the low-frequency region of the IR spectrum (as indeed expected) nor are clearly detectable absorptions found in the same region of the Raman spectrum (Figure 4). (b) One medium-to-strong absorption is clearly observable at 381 cm^{-1} for **I** (Figure 2), which apparently does not change its position for the ^{15}N-containing sample. At the same time, a weak-to-medium absorption is found in the Raman spectrum of **I** at 396 cm^{-1}, which is in a region free from other absorptions. Unfortunately, the assignment of this band as ν_s(Mn−N−Fe) cannot be direct, because the mechanism through which it can becomes IR active cannot be easily identified. Nevertheless, some connection with the Mn−N−Fe-bridged system clearly exists, since this absorption disappears, along with the doublet at 956−945 cm^{-1} (ν_{as}(Mn−N−Fe)) when **I** is oxidized by perchloric acid to its corresponding mono(perchlorate) form, **I**-ClO_4. These spectral changes are reversible, and both the doublet and the 380 cm^{-1} absorption re-appear upon reduction of **I**-ClO_4 with $NaBH_4$ to give **I** (see Experimental Section).

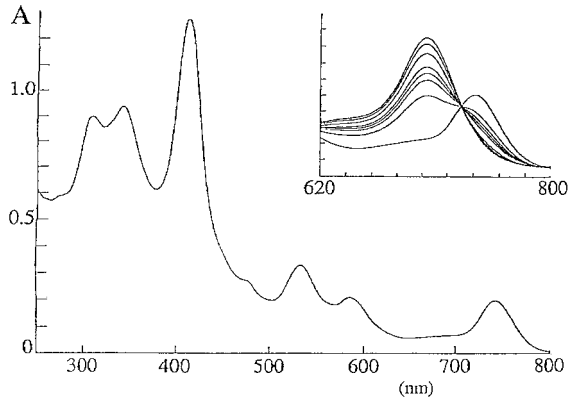

Figure 5. UV−visible solution spectrum of **I** in CH_2Cl_2 and equilibrium spectra (inset) in the same solvent in the presence of different pyridine concentrations (range 5 × 10^{-5}−5.3 × 10^{-3} M).

This behavior lends further support to an assignment of the 381 cm^{-1} absorption as ν_s(Mn−N−Fe).

(iii) Interaction of I with Pyridine and Formation of the Monoadduct, I-py. The mono(pyridine) adduct of **I** was isolated in the solid state. This compound has an IR spectrum which closely resembles that of **I** except for the presence of weak additional absorptions due to pyridine, a shift of ν_{as}(Mn−N−Fe) to lower frequencies (942, 925 cm^{-1}), and a nearly complete disappearance of the 381 cm^{-1} band. The Mössbauer spectrum of **I**-py shows an isomer shift value which is slightly lower than that of **I** (Table 1), whereas the ΔE_Q value is practically unchanged. The δ value of this compound indicates an increased positive charge on the Fe center and hence a more balanced charge distribution in the Mn−N−Fe moiety. However, despite this information, the specific metal ion which is coordinated by a pyridine molecule cannot be unambiguously assigned.

The UV−visible spectrum of **I** in CH_2Cl_2 is unchanged for 1−2 h (Figure 5)(nm ($10^{-4}\epsilon$): 309 (5.9); 343 (6.2); 412 (8.4); 534 (2.2); 585 (1.4) and 742 (1.3)). The conversion of **I** to **I**-py was followed spectrophotometrically in CH_2Cl_2 upon addition of pyridine. The spectral changes were monitored between 800 and 250 nm and suggest the formation of a pyridine adduct, on the basis of the following equation:

$$\mathbf{I} + n\ \mathrm{py} \rightleftarrows \mathbf{I}\text{-}(\mathrm{py})_n \qquad (1)$$

for which the equilibrium constant is expressed as

$$K = [\mathbf{I}\text{-}(\mathrm{py})_n]/[\mathbf{I}][\mathrm{py}]^n$$

which can be converted into the expression

$$\log[(A - A_0)/(A_f - A)] = \log K + n \log [\mathrm{py}] \qquad (2)$$

where A_0, A, and A_f are, at a fixed wavelength, the absorption in the absence of py, at a given py concentration, and at saturation, respectively, and n is the number of pyridine molecules ligated by **I**. The range of pyridine concentrations examined was between 5 × 10^{-5} and 5.3 × 10^{-3} M.

The binding of pyridine to **I** is slow, and the spectral changes observed after each py addition required several minutes to reach equilibrium. Several isosbestic points are observed in the region explored and are located at 730, 531, 432, and 403 nm, being in agreement with the simple process given in eq 1. The equilibrium spectra between 620 and 800 nm are given in Figure 5 (inset), while Figure 6 shows the plot of $\log[(A - A_0)/(A_f - A)]$ versus log [py]. The plot is linear and has a slope of

(17) Cleare, M. J.; Griffith, W. P. *J. Chem. Soc. A* **1970**, 1117.
(18) Rossi, G.; Gardini, M.; Pennesi, G.; Ercolani, C.; Goedken, V. L. *J. Chem. Soc., Dalton Trans.* **1989**, 193.
(19) Schick, G. A.; Bocian, D. F. *J. Am. Chem. Soc.* **1983**, *105*, 5, 1830.

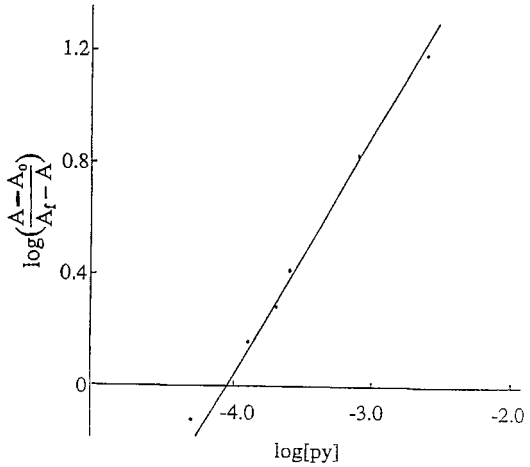

Figure 6. Plot of $\log(A - A_0)/(A_f - A)$ vs log [py] (slope 0.90).

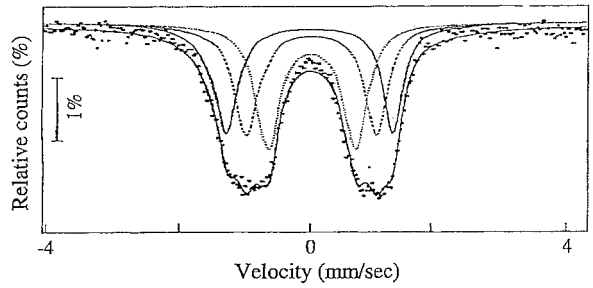

Figure 7. Low-temperature (78 K) Mössbauer spectrum of **I**-ClO_4.

0.90, consistent with formation of a 1:1 py adduct ($n = 1$), effectively giving the same **I**-py compound which was isolated and characterized in the solid state. The calculated K value for eq 1 is ca. 1.0×10^4.

(iv) Characterization of I-ClO_4 and [I-$(py)_2$](ClO_4). **I**-ClO_4 exhibits an IR spectrum which has an intense absorption at 1095 cm^{-1} due to the presence of ClO_4^-. The doublet at 956 and 945 cm^{-1} (ν_{as}(Mn−N−Fe)) for the inital complex is no longer present nor is the 381 cm^{-1} band detected. Its Mössbauer spectrum is shown in Figure 7, and the related data are given in Table 1 (complex **11**). The spectrum can be interpreted by assuming the presence of three overlapping doublets indicating the presence of three different Fe-containing species which are labeled as **11** (34%), **11′** (29%), and **11″** (37%). All three components of the material show isomer shifts close to zero, clearly suggesting that all three species contain Fe(IV). This result can be interpreted in terms of a single metal-centered oxidation which results in formation of three closely related Mn(IV)−Fe(IV) (d^7) couples.

The EPR spectrum of **I**-ClO_4 is given in Figure 8. It shows a clean well-resolved hyperfine structure which indicates the presence of one unpaired electron spending its time along the Mn−N−Fe bridge. No signals corresponding to the presence of organic radicals are observed, thus confirming that the one-electron oxidation is metal rather than ligand-centered. It is noteworthy to point out that the absence of signals attributable to organic radicals also excludes the possibility that a ligand-centered oxidation has taken place concomitantly with the metal-centered oxidation (a two-electron oxidation). It should also be emphasized that the observed spectrum is quite peculiar, since it is associated with a very rare bimetallic moiety. The hyperfine structure of the spectrum unequivocally establishes the interaction of the unpaired electron with the nuclear spin of Mn (natural abundance 100% ^{55}Mn, nuclear spin $^5/_2$). The g and A values calculated from the spectrum are as follows: $g_{||} = 1.980$, $g_\perp = 2.038$, $A_{||} = 179$ G, $A_\perp = 64.5$ G. From the large A values observed, it can be concluded that the unpaired electron is mainly located on the Mn ion.

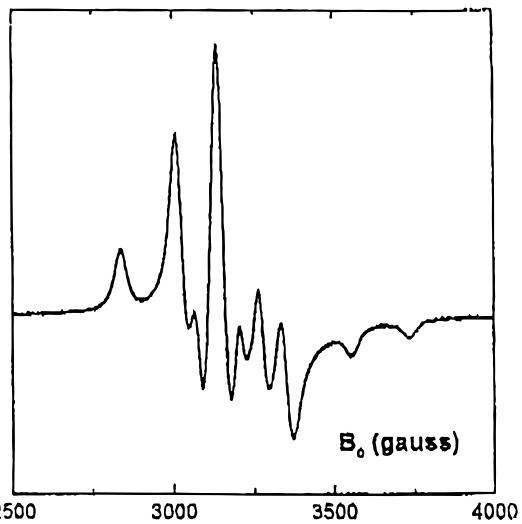

Figure 8. Low-temperature (78 K) ESR spectrum of **I**-ClO_4.

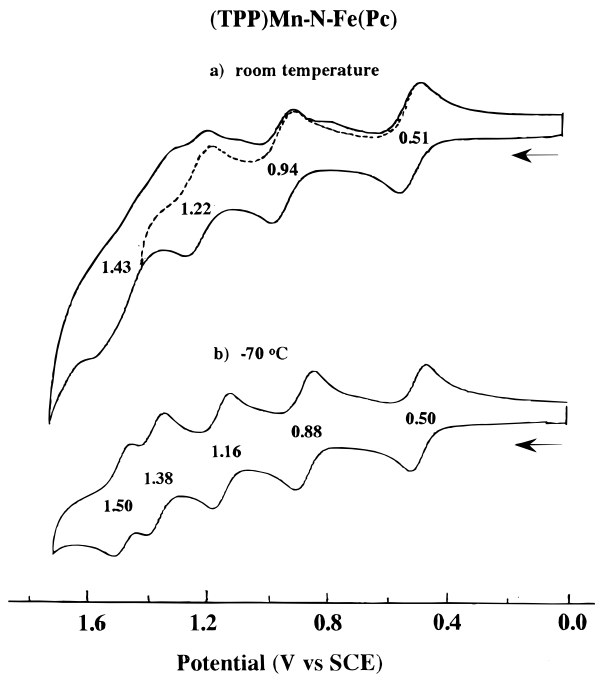

Figure 9. Cyclic voltammograms of **I** in CH_2Cl_2, 0.1 M TBAP (a) at room temperature and (b) at −70 °C.

[**I**-$(py)_2$](ClO_4) (complex **12** in Table 1) shows a Mössbauer spectrum with a clean doublet having δ and ΔE_Q values close to one of the three components of **I**-ClO_4 (complex **11″**). The isomer shift value is therefore also indicative of the presence of Fe(IV) which confirms the metal-centered oxidation as in the case of **I**-ClO_4.

An Fe(IV)−Fe(IV) couple is certainly present in the species formed by oxidation of **II** with $HClO_4$ to give **II**-ClO_4, as clearly indicated by the measured isomer shift value (complex **13** in Table 1) which is in line with the δ value of the singly oxidized species from **II** already discussed in a previous publication.[4]

(v) Electrochemistry in Neat CH_2Cl_2 and Pyridine. Cyclic and differential pulse voltammetric experiments were carried out for **I** in both CH_2Cl_2 and pyridine containing 0.1 M TBAP, and the results of these experiments are shown in Figures 9 and 10. The oxidations are best defined in CH_2Cl_2, and the

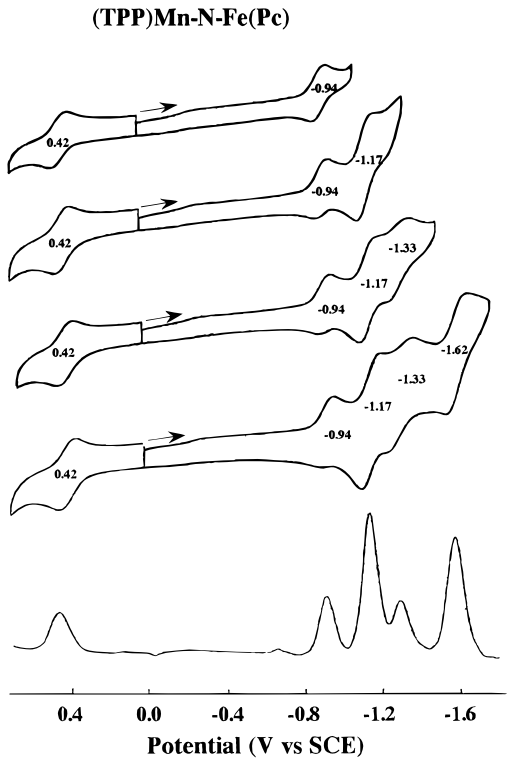

Figure 10. Cyclic and differential pulse voltammograms of **I** in py containing 0.1 M TBAP.

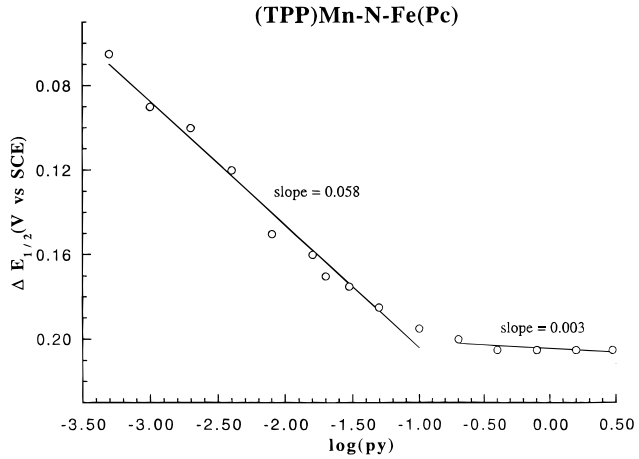

Figure 11. Plot of $\Delta E_{1/2}$ vs log [py] for the first oxidation of **I.**

reductions are best defined in pyridine. The room-temperature experiments in CH_2Cl_2 show three one-electron oxidations at 0.51, 0.94, and 1.22 V, plus two partially overlapped oxidations located at 1.43 V. Five well-defined one-electron oxidations are observed at −70 °C (Figure 9), and these occur at $E_{1/2}$ = 0.50, 0.88, 1.16, 1.38, and 1.50 V. Four redox processes are observed for reduction of **I** in pyridine (see Figure 10), and thus a total of nine redox processes can be seen without cleavage of the Fe−N−Mn bond. The additional redox reactions are now under further investigation, and attempts are being made to isolate several of the mixed-ligand bimetallic complexes in both high and low oxidation states.

(vi) Electrochemistry in CH_2Cl_2/Pyridine Mixtures. Half-wave potentials for the first oxidation of **I** in CH_2Cl_2/pyridine mixtures are dependent upon the concentration of pyridine in solution. The shift in the reversible $E_{1/2}$ values upon going from neat CH_2Cl_2 to different CH_2Cl_2/pyridine mixtures is shown in Figure 11. The initial slope of the $\Delta E_{1/2}$ vs log [py] plot is 58 mV which can be interpreted in terms of reaction 3, while the slope is 3 mV at higher pyridine concentrations which can be interpreted in terms of reaction 4.

$$\mathbf{I}\text{-(py)} + \text{py} \rightleftarrows [\,\mathbf{I}\text{-(py)}_2]^+ + e^- \quad (3)$$

$$\mathbf{I}\text{-(py)}_2 \rightleftarrows [\,\mathbf{I}\text{-(py)}_2]^+ + e^- \quad (4)$$

Formation constants were calculated for **I**-py_2 and [**I**-py_2]$^+$ using the electrochemical data and standard equations[20] relating half-wave potentials for ligated and unligated metal complexes. The relevant ligand binding reactions are given in eqs 5 and 6.

$$\mathbf{I} + 2\text{py} \rightleftarrows \mathbf{I}\text{-(py)}_2 \quad \log \beta_2 = 4.05 \quad (5)$$

$$[\mathbf{I}]^+ + 2\text{py} \rightleftarrows [\,\mathbf{I}\text{-(py)}_2]^+ \quad \log \beta_2 = 7.54 \quad (6)$$

The data are self-consistent and, in the case of [**I**-py_2]$^+$, can be compared to a $\log \beta_2 = 6.44$ for the addition of two pyridine molcules to [(TPP)Fe−C−Fe(TPP)]$^+$ in benzonitrile.[21]

Acknowledgment. C.E. and K.M.K. acknowledge the financial support for exchange visits by the University of "La Sapienza" and the Houston University through a bilateral exchange program. Financial support from the Robert A. Welch Foundation (K.M.K., Grant E-680) is also gratefully acknowledged. The authors are very grateful to Prof. P. Deplano (University of Cagliari), Dr. D. Attanasio (Area della Ricerca, CNR), and Dr. Eric Van Caemelbecke for useful discussions on the electrochemistry, Raman, and EPR spectra. Thanks are addressed to Mr. G. D'Arcangelo (University of Tor Vergata, Roma) for FAB measurements, to Dr. P. Galli (Chemistry Department, University "La Sapienza") for C, H, and N elemental analyses, to Dr. R. Dragone for quantitative detection of Mn and Fe by atomic absorption, and to Mrs. Xiaoyu Tan for help with the electrochemical measurements.

IC971585+

(20) Kadish, K. M. Iron Porphyrins, *Part Two*; Lever, A. B. P., Gray, H. B., Eds.; Addison-Wesley Publishing Co.: Reading, MA, 1983; pp 161−243.

(21) Lancon, D.; Kadish, K. M. *Inorg. Chem.* **1984**, *23*, 3942.